Every Combinatorial Polyhedron Can Unfold with Overlap

Joseph O'Rourke
Smith College, Northampton, MA, USA

Abstract

Ghomi proved that every convex polyhedron could be stretched via an affine transformation so that it has an edge-unfolding to a net [5], a non-overlapping planar polygon. One can view his result as establishing that every combinatorial polyhedron $\mathcal{P}$ has a metric realization P that allows unfolding to a net.

Joseph Malkevitch asked if the reverse holds (in some sense of "reverse"): Is there a combinatorial polyhedron $\mathcal{P}$ such that, for every metric realization P in $\mathbb{R}^3$, and for every spanning cut-tree T of the 1-skeleton, P cut by T unfolds to a net? In this paper we prove the answer is NO: Every combinatorial polyhedron has a realization and a cut-tree that edge-unfolds the polyhedron with overlap.

Keywords and phrases convex polyhedra, unfolding, edge-unfolding, net, overlap, Dürer's problem

Digital Object Identifier 10.57717/cgt.v4i2.54

1 Introduction

Joseph Malkevitch asked[1] whether there is a combinatorial type $\mathcal{P}$ of a convex polyhedron P in $\mathbb{R}^3$ whose every edge-unfolding results in a net. One could imagine, to use his example, that every realization of a combinatorial cube unfolds without overlap for each of its 384 spanning cut-trees [17].[2] The purpose of this paper is to prove this is, alas, not true: Every combinatorial type can be realized and edge-unfolded to overlap: Theorem 1 (Section 3). For an overlapping unfolding of a combinatorial cube, see ahead to Fig. 12.

The motivation for this work is Dürer's Problem, which asks whether every convex polyhedron has a non-overlapping edge-unfolding. This question was raised 50 years ago [15], but a positive answer has been assumed for 500 years, starting with the work of Albrecht Dürer. Despite considerable effort by researchers [7], the question remains open, with only narrow classes of polyhedra proved to edge-unfold without overlap.

One of the strongest results in this area was obtained by Ghomi, who proved that every convex polyhedron P could be stretched via an affine transformation so that it has an edge-unfolding to a net [5]. Malkevitch asked if there is some combinatorial type of polyhedron $\mathcal{P}$ whose every metric realization P always avoids overlap for all of its spanning trees. The main result of this paper is to answer Malkevitch's question NO: every $\mathcal{P}$ has a realization P and a spanning tree T so that $P \setminus T$ overlaps. An implication of this result, together with [5], is that a resolution of Dürer's Problem must focus on the geometry rather than the combinatorial structure of convex polyhedra.

1.1 Proof outline

The overall structure of the proof is as follows:

$$G \equiv \mathcal{P} \to P \to \bar{P} \to \text{Unfold/Overlap}.$$

[1] Personal communication, Dec. 2022.
[2] Burnside's Lemma can show that these 384 trees lead to 11 incongruent non-overlapping unfoldings of the cube [6].

The combinatorial polyhedron $\mathcal{P}$ is given by a 3-connected planar graph G. Tutte embedding and Maxwell-Cremona lifting maps $\mathcal{P}$ to a convex polyhedron $P \subset \mathbb{R}^3$. We then modify P by an affine transformation to $\bar{P}$. A particular spanning cut tree T then unfolds $\bar{P}$ with overlap, i.e., flattening $P \setminus T$ results in a non-simple polygon, one sharing interior points.

We next offer preliminaries defining terms and describing tools we will employ.

2 Preliminaries

A *convex polyhedron* P is the convex hull of a finite number of points in $\mathbb{R}^3$. The 1-*skeleton* of P is the metric graph formed by its vertices and edges. A *combinatorial polyhedron* $\mathcal{P}$ is given by its 3-connected planar graph G, without metric information. By *Steinitz's theorem*, G is the 1-skeleton of a convex polyhedron. A *Schlegel diagram* is a representation of a combinatorial polyhedron as a plane graph. See ahead to Fig. 1 for an example.

The curvature at points of P is concentrated at its vertices. The *discrete Gaussian curvature* at a vertex v is the *angle gap* at v, 2π minus the incident face angles. The *Gauss map* connects the curvature to face normals. Let $\mathbb{S}$ be the unit-radius *Gaussian sphere*.

▶ **Proposition 0.** *The discrete Gaussian curvature at a vertex v is the area of the geodesic polygon on $\mathbb{S}$ determined by the normals to the faces incident to v.*

See [16] or [1], or ahead to Fig. 10 for an example. Henceforth we abbreviate "discrete Gaussian curvature" to *curvature*.

The Maxwell-Cremona correspondence connects a straight-line graph G embedded in the plane to its lifting. A *lifting* is an assignment of heights to the vertices such that the vertices of every face are coplanar. A *convex lifting* must satisfy in addition that each edge shared by two faces is convex. An *equilibrium stress* on a graph G is an assignment of weights to each edge of G, which, when interpreted as forces, induce an equilibrium (sum to zero) at every vertex. The Maxwell-Cremona correspondence says that a plane graph with an equilibrium stress of positive weights lifts to a convex polyhedron. See ahead to Fig. 2 for an example.

We will not need details of this correspondence, but only that *Tutte's theorem* [19] determines a positive equilibrium stress for a given plane graph G, which then leads to a convex lifting, i.e., to a convex polyhedron [12, p. 117].

Finally, we turn to *Dürer's problem*, which asks whether every convex polyhedron has an edge-unfolding that avoids overlap [7]. An *edge-unfolding* is an unfolding (development) of a polyhedron to a polygon in the plane by cutting a spanning tree of its 1-skeleton and flattening. We distinguish between *strong overlap* when the unfolding shares interior points, and *weak overlap* where the boundary of the polygon may touch but not cross itself. An edge-unfolding that avoids strong overlap is called a *net*, a *weakly simple polygon* [2]. An unfolding that avoids weak overlap is a *simple polygon*—a Jordan curve.

3 Main theorem

The main result of this paper can now be stated:

▶ **Theorem 1.** *Any combinatorial convex polyhedron $\mathcal{P}$, given by a 3-connected planar graph G, can be realized as a convex polyhedron P in $\mathbb{R}^3$ whose 1-skeleton has a spanning cut-tree T such that the edge-unfolding of $P \setminus T$ strongly overlaps in the plane.*

3.1 Proof case structure

The proof consists of four cases, the first of which is in some sense the generic case. All the cases depend on a pair of faces, B and F, where B becomes the base face of P, and F contains (or is equal to) a triangle $\triangle$, the *overlap triangle*. Case 1 applies whenever there is a pair of faces B, F of disjoint faces (i.e., they share no vertices) and F is a triangle, $F = \triangle$. Here the proof is simple and intuitive. The other three cases have special conditions, and their proofs are less straightforward. We list the other conditions before focusing on Case 1.

Case 1. There is a pair of disjoint faces B, F with F a triangle.
Case 2. There are pairs of disjoint faces B, F, but no pair includes a triangle.
Case 3. There are no pairs of disjoint faces, but there is a pair of faces B, F that share a single vertex.
Case 4. Every pair of faces shares two or more vertices, which implies that each pair of faces shares an edge.

Every convex polyhedron falls into one of these cases. Although we will see that all but Case 4 can be proved by the same arguments, we opt to argue intuitively that Case 1 can be settled by an especially simple approach.

4 Case 1

We describe the proof plan for Case 1 in the form of a multi-step algorithm. We will see that only step (5) and (6) need be altered to cover the cases beyond Case 1. We will illustrate the steps with an icosahedron before providing details.

Case 1 Algorithm. Realizing G to unfold with overlap.
Input: A 3-connected planar graph G.
Output: Polyhedron $\bar{P}$ realizing G and a cut-tree T that unfolds P with overlap.

(1) Identify disjoint faces B, F, with $F = \triangle$ a triangle.
(2) Embed B as a convex polygon in the plane.
(3) Apply Tutte's theorem to calculate a positive equilibrium stress for G.
(4) Apply Maxwell-Cremona lifting of the stressed G to a convex polyhedron P.
(5) Compress $P \to \bar{P}$ vertically to reduce curvatures of $\triangle$'s vertices (if necessary).
(6) Label $\triangle = a_1a_2a_3$ to satisfy several conditions (to be described).
(7) Form cut-tree T, including 2-edge path $\Lambda = a_1a_2a_3$ around $\triangle$.
(8) Unfold $P \setminus T \to$ Overlap.

We are given a 3-connected planar graph G, which constitutes the combinatorial type of a convex polyhedron. By Steinitz's theorem, we know G is the 1-skeleton of a convex polyhedron.

(1) Identify disjoint faces B, F, with with $F = \triangle$ a triangle. This is the assumption that constitutes Case 1.

The next three steps realize G with a convex polyhedron P.

(2) Embed B as a convex polygon in the xy-plane. Select coordinates for the vertices of B, which then pin B to the plane. B must be convex, but otherwise its shape is arbitrary.

(3) Apply Tutte's theorem [19] to calculate an equilibrium stress—positive weights on each edge of G—that, when interpreted as forces, induce an equilibrium (sum to zero) at every vertex. This provides explicit coordinates for all vertices interior to B. The result is a Schlegel diagram, with all interior faces convex regions, and all nonbase vertices strictly interior to B. Fig. 1 illustrates this for the icosahedron.[3]

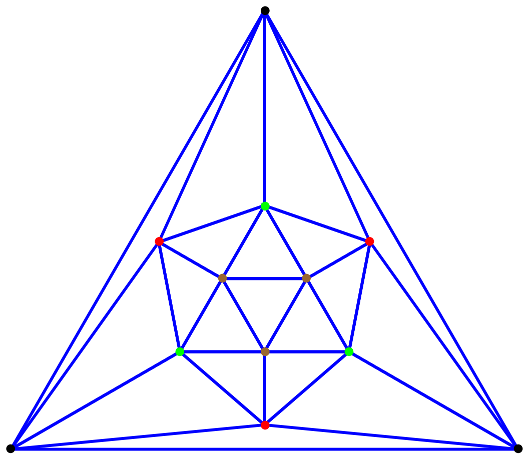

Figure 1 Icosahedron Schlegel diagram. The outer triangle is base B.

(4) Apply Maxwell-Cremona lifting to P. The Maxwell-Cremona theorem says that any straight-line planar drawing with an equilibrium stress has a polyhedral lifting via a "reciprocal diagram." The details are not needed here;[4] we only need the resulting lifted polyhedron P. An example from [13], Fig. 2, shows the vertical z-lifting of a Schlegel diagram of the dodecahedron. A z-lifting of the vertices of the icosahedron in Fig. 1 is shown in Fig. 3.[5]

After the lifting, we have realized $\mathcal{P}$ with a polyhedron P that has the particular structure of a base into which all non-base vertices project.

(5) z-compress $P \to \bar{P}$ vertically to reduce curvatures of $\triangle$'s vertices (if necessary). Not needed in icosahedron example, but guaranteed by Lemma 4 below.
(6) Label $\triangle = a_1a_2a_3$ satisfying several conditions (to be described).
(7) Form cut-tree T, including the 2-edge path $\Lambda = a_1a_2a_3$ around $\triangle$, with $\deg(a_1) = 1$ and $\deg(a_2) = 2$. We can think of a_1 as the root of the spanning tree, which includes the Λ-shaped (red) path $a_1a_2a_3$ around $\triangle$. The remainder of T is completed arbitrarily.
(8) Unfold $P \setminus T$. Finally, the conditions on $\triangle$ ensure that cutting T unfolds P with overlap in the vicinity of a_2. See Fig. 5.

4.1 Loose overlap conditions

We continue to focus on Case 1, when $\triangle$ is disjoint from B. The following are sufficient conditions to guarantee overlap, and each is achievable (Lemma 3). (Other cases will need a tightening of these conditions.) Let ω_i denote the curvature at vertex a_i.

[3] Here the drawing is approximate, because I did not explicitly calculate the equilibrium stresses.
[4] A good resource on this topic is [12].
[5] This is again an approximation as I did not calculate the reciprocal diagram.

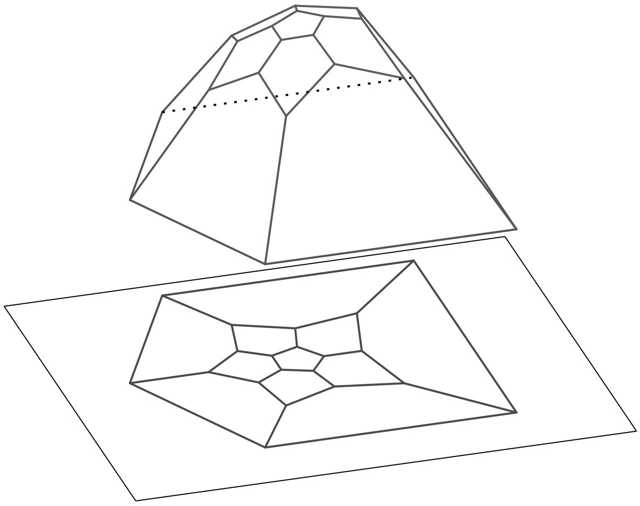

Figure 2 Maxwell-Cremona lifting of a dodecahedral diagram. [13], by permission of author.

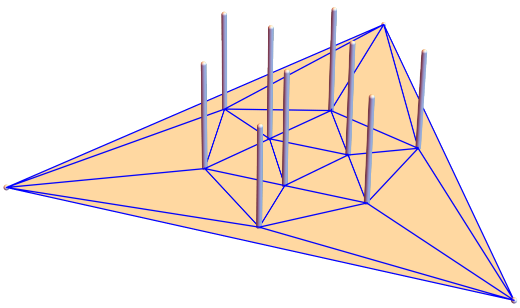

Figure 3 Vertical z-lifting the vertices of the icosahedron Schlegel diagram in Fig. 1.

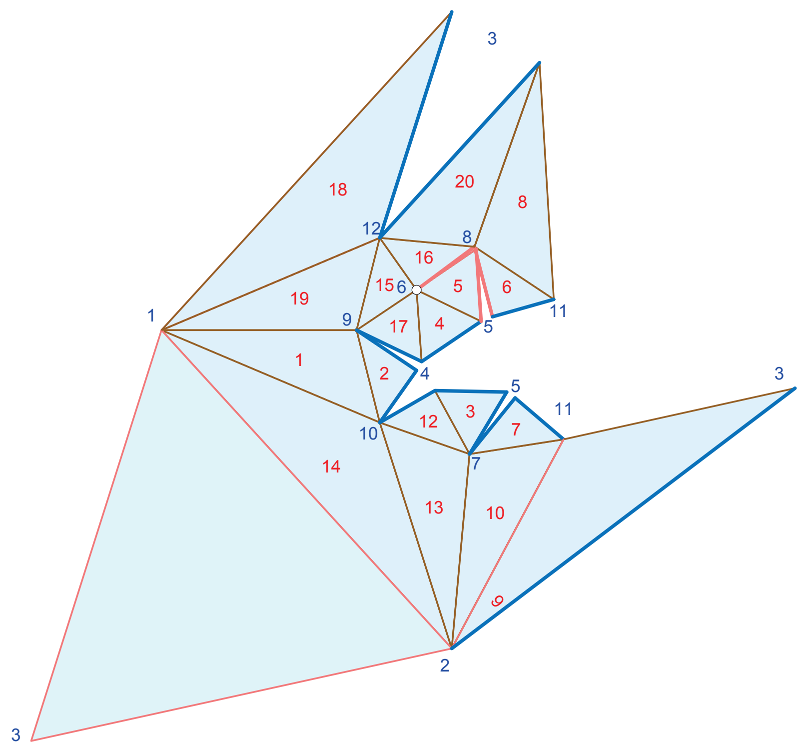

Figure 4 Red: face numbers; blue: vertex indices. Face 5 is $\triangle$. Λ-portion of spanning tree T red; remainder blue.

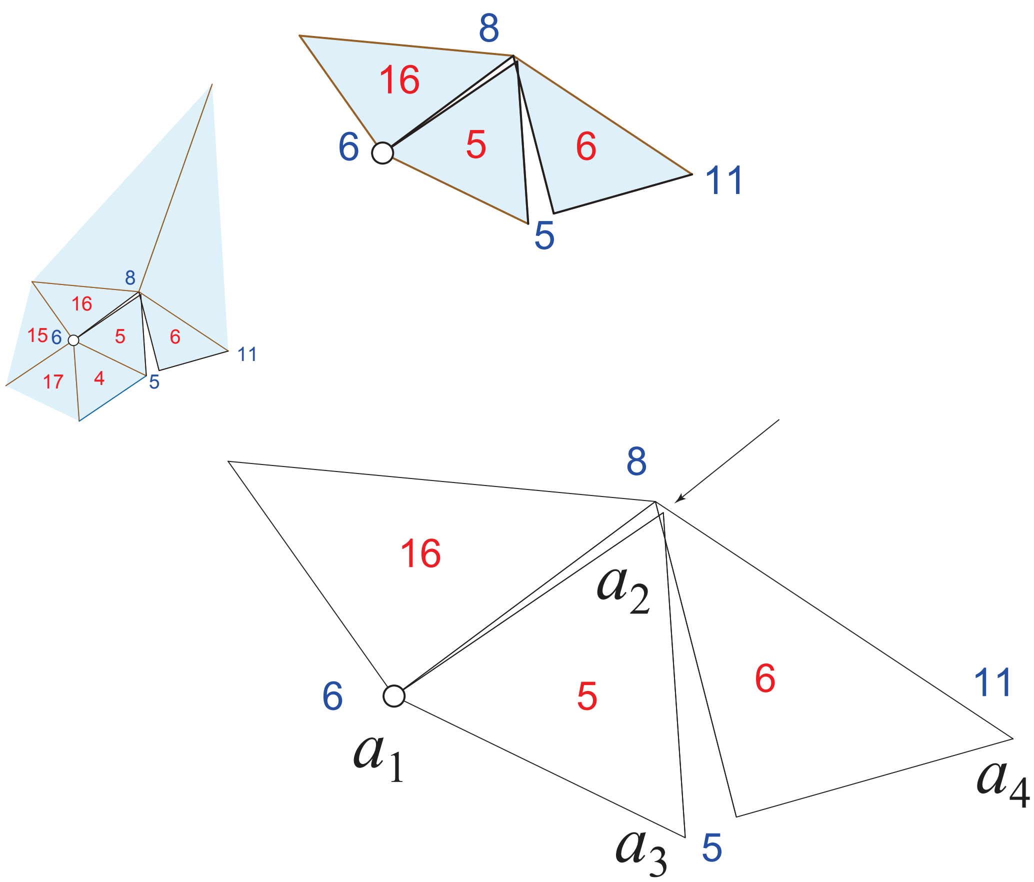

Figure 5 Close-up views of overlap.

▶ **Lemma 2** (Loose Overlap Conditions). *If the following five conditions are satisfied for $\triangle = a_1a_2a_3$, cutting T guarantees overlap:*

(a) $\triangle$ *is disjoint from* B.
(b) With $\omega = \max(\omega_1, \omega_2)$, $\omega < 20°$.
(c) With α *the angle of* $\triangle$ *at* a_2, $\alpha \le 60°$.
(d) The lengths ratio $r = \frac{|a_2a_3|}{|a_1a_2|}$ *satisfies* $r \ge 1$.
(e) The cut-tree T *includes the* 2*-edge path* $\Lambda = a_1a_2a_3$, *with* $\deg(a_1) = 1$ *and* $\deg(a_2) = 2$.

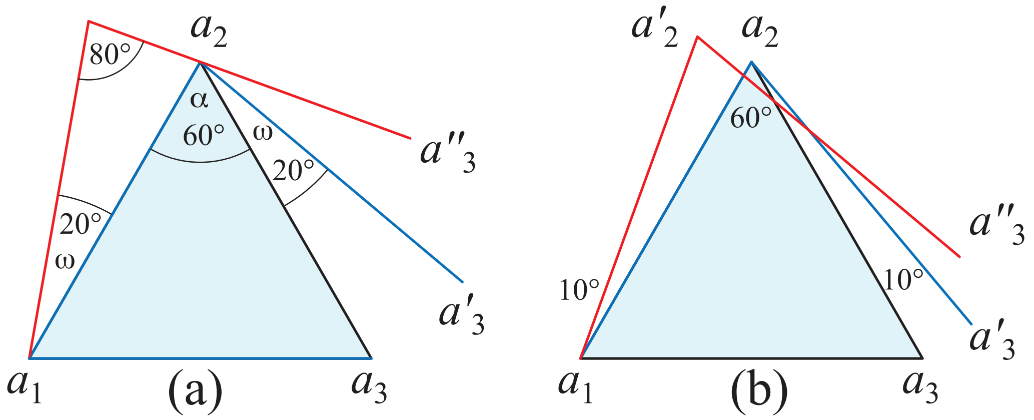

Figure 6 (a) $\alpha = 60°$ and $\omega = 20°$ just avoids overlap—only grazing contact, whereas (b) $\omega = 10°$ (strongly) overlaps.

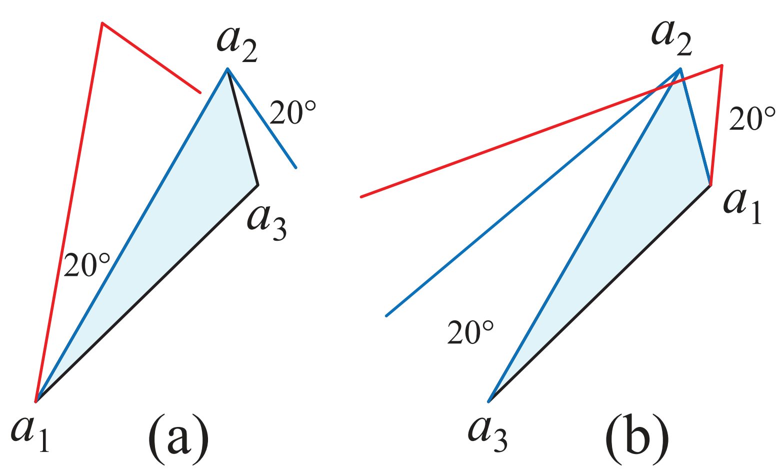

Figure 7 $\alpha = 45°$, $\omega = 20°$. (a) small r (0.3) avoids overlap. (b) Relabeling so that r is larger (> 3) guarantees overlap.

Proof. *Sketch.* We use Fig. 6 to explain why these conditions lead to overlap. By the conditions on T, no other edge of T is incident to either a_1 or a_2. Embedding a neighborhood of an interior point of $\triangle$ fixed in the plane, the flattening of a_1 and a_2 to the plane can be viewed as first turning the edge a_2a_3 by (at most) ω about a_2, moving vertex a_3 to a'_3, and then rotating the rigid path $a_1a_2a_3'$ about a_1 by (at most) ω. An elementary calculation shows that $\omega = 20°$ would just barely avoid overlap when α is at its largest (60°): Fig. 6(b).

So when the curvatures ω_1, ω_2 at a_1, a_2 are both strictly less than $\omega = 20°$, and $r \geq 1$, (strong) overlap occurs. The role of the ratio r is illustrated in Fig. 7: small r could avoid overlap (a), but relabeling enlarges r and guarantees overlap (b).

The reason we label this a *Sketch* is that the claim that overlap occurs under these conditions requires a more formal proof, a proof provided later in Lemma 5. ◀

In the unfolded icosahedron in Fig. 4, the angle at a_2 is $\approx 59°$, and the curvatures ω_1, ω_2 at a_1, a_2 are approximately 2° and 8° respectively. So Lemma 2 is satisfied.

The basic reason these conditions "work" to create overlap is that the cut-path Λ around $\triangle$ is not *radially monotone*, a concept introduced in [8] and used in [9] and [11] to avoid overlap.

Now we show that the five conditions are achievable:

▶ **Lemma 3** (Loose Conditions Achievable). *The five conditions in Lemma 2 are achievable in Case 1.*

Proof.

(a) $B, \triangle$ are disjoint by assumption in Case 1.
(b) That the curvatures ω_1, ω_2 are both strictly less than $\omega = 20°$ is achieved by the vertical z-compression step (5), Lemma 4 below.
(c) The angle $\alpha \leq 60°$ is achieved by labeling (step (6)) the minimum angle of $\triangle$ to be at vertex a_2.
(d) The lengths ratio $r \geq 1$ is achieved by choosing the labeling of a_1 and a_3 so that edge a_2a_3 is at least as long as edge a_1a_2; see again Fig. 7.
(e) We have the freedom to select the cut-tree T so that T includes the 2-edge path $\Lambda = a_1a_2a_3$, with $\deg(a_1) = 1$ and $\deg(a_2) = 2$.

◀

4.2 Vertical z-compression

We now justify step (5): $P \to \bar{P}$. Recall B lies in the xy-plane. Define *vertical z-compression* as scaling the z-coordinate of each vertex by $0 < s_z < 1$: $(x, y, z) \to (x, y, s_z\, z)$.

▶ **Lemma 4.** *Vertical z-compression reduces the curvature $\omega(v)$ at any interior (non-base) vertex v below any given threshold ω.*

Proof. Let a_1, a_2, a_3 be a triangle of P incident to v, with $v = a_2$. Without loss of generality, translate P so that a_2 is placed at the origin, and scale the z-coordinates of every vertex by $s_z \in [0, 1]$:

$$
\begin{aligned}
a_1 &= (a_{1x}, a_{1y}, s_z\, a_{1z}) \\
a_2 &= (0, 0, 0) \\
a_3 &= (a_{3x}, a_{3y}, s_z\, a_{3z})
\end{aligned}
$$

The normal vector to the triangle at a_2 is

$$
\begin{aligned}
\hat{n} &= (a_2 - a_1) \times (a_2 - a_3) \\
&= (s_z\, c_x, s_z\, c_y, c_z)
\end{aligned}
$$

where c_x, c_y, c_z are constants in the coordinates of the three vertices. Because the z-component c_z of $\hat{n}$ is unaffected by s_z, $\hat{n} \to (0, 0, c_z)$ as $s_z \to 0$, i.e., the normal vector approaches pointing vertically, parallel to the z-axis.

Because this is true for all triangles sharing the vertex $v = a_2$, all the normals of these incident triangles approach parallelism with the z-axis. The Gauss map of these normals then encloses a vanishing area on $\mathbb{S}$. Therefore, by Proposition 0, the curvature at v approaches zero, and selection of a sufficiently small s will reduce the curvature at v below any given ω. ◀

5 Cases 2 and 3

The assumptions of Case 1—that there are two disjoint faces B, F, with F a triangle—allowed us to achieve both $\alpha \le 60°$ and $r \ge 1$ by z-compression in step (5) and then appropriate choice of labeling $\triangle = a_1a_2a_3$ in step (6).

We first describe Case 2 and Case 3 at a high level and what each needs to establish.

Case 2 retains disjointness, but no pair B, F includes a triangle F, so the analog of α could be large. For example, no face angle in Fig. 2 is $\le 60°$. Label three consecutive vertices of F as $\triangle = a_1a_2a_3$. The angle α at a_2 might need to be reduced.

In Case 3, no pair of faces are disjoint, but there is a pair B, F that share a single vertex v. (Whether or not F is a triangle is not relevant to this case.) We must arrange that v plays the role of a_3 in $\triangle a_1a_2a_3$, because only the curvatures at a_1, a_2 need be small; the curvature at a_3 might be large. With a_3 identified with v, there is no possibility of relabeling to achieve a large r ratio (Fig. 7).

We will establish overlap in both Cases 2 and 3 (and later Case 1) by x-stretching rather than z-compression, stretching that will satisfy a tighter sufficiency lemma.

5.1 Tighter overlap conditions

▶ **Lemma 5** (Tighter Sufficiency). *If the following five conditions are satisfied for $\triangle = a_1a_2a_3$, cutting T guarantees overlap:*

(a) a_1 and a_2 are disjoint from B. (But a_3 could be a vertex of B.)
(b) With $\omega = \max(\omega_1, \omega_2)$, $\omega < 20$.
(c) With α the angle of $\triangle$ at a_2, $\alpha + 3\omega/2 < 90°$.
(d) With $|a_1a_2| = 1$ so that $r = |a_2a_3|$, $r > \sin(\omega)/\sin(\alpha + 2\omega)$.
(e) The cut-tree T includes the 2-edge path $\Lambda = a_1a_2a_3$, with $\deg(a_1) = 1$ and $\deg(a_2) = 2$.

Proof. The five conditions parallel those in Lemma 2.

(a) Reflects the assumptions of Case 2 and 3.
(b) The limit on ω_1, ω_2 is the same as in Lemma 2: $\omega_{\max} = 20°$.
(c) The point of the constraint $\alpha + 3\omega/2 < 90°$ is more evident if we define $\beta = 90° - (\alpha + 3\omega/2)$. Then $\beta > 0$ says that, in the notation of Fig. 8, $a_2'a_3''$ is turned clockwise about a_2' from $a_2'a_2$. If β were negative, then overlap would be avoided. (Note that if $\alpha, \omega = 60°, 20°$ as in Lemma 2, $\alpha + 3\omega/2 = 90°$ so $\beta = 0$—just touching as in Fig. 6(a).)
(d) The ratio r must be sufficient for $a_2'a_3''$ to cross a_1a_2. If r is too short, as we've seen (Fig. 7) crossing/overlap could be avoided, and, unlike in Case 1, we may not have the freedom to relabel a_1 and a_3 to achieve long-enough r.

Scaling so that $|a_1a_2| = 1$ is no loss of generality and simplifies the algebra: now the ratio $r = |a_2a_3|$. Let b be the length of a segment from a_2', along the direction $a_2'a_3''$, that crosses a_1a_2 at a point t; see Fig. 8(b). Note that $\angle a_1, t, a_2' = \pi - (\alpha + 2\omega)$, and so by the triangle law of sines, $b = \sin(\omega)/\sin(\alpha + 2\omega)$. Thus the constraint $r > b$ ensures that $a_2'a_3''$ crosses a_1a_2.

The expression $\sin(\omega)/\sin(\alpha + 2\omega)$ achieves its maximum[6] when $\alpha = 0$ and $\omega = \omega_{\max} = 20°$, the latter by (b) above. Calculation leads to $b_{\max} \approx 0.53$.

(e) As in Lemma 2, we have the freedom to select the cut-tree T so that $\deg(a_1) = 1$ and $\deg(a_2) = 2$. Then the rotations depicted in Fig. 8 accurately describe the unfolding in the vicinity of a_2, and (strong) overlap is guaranteed because $\beta > 0$ and $r > b$.

◀

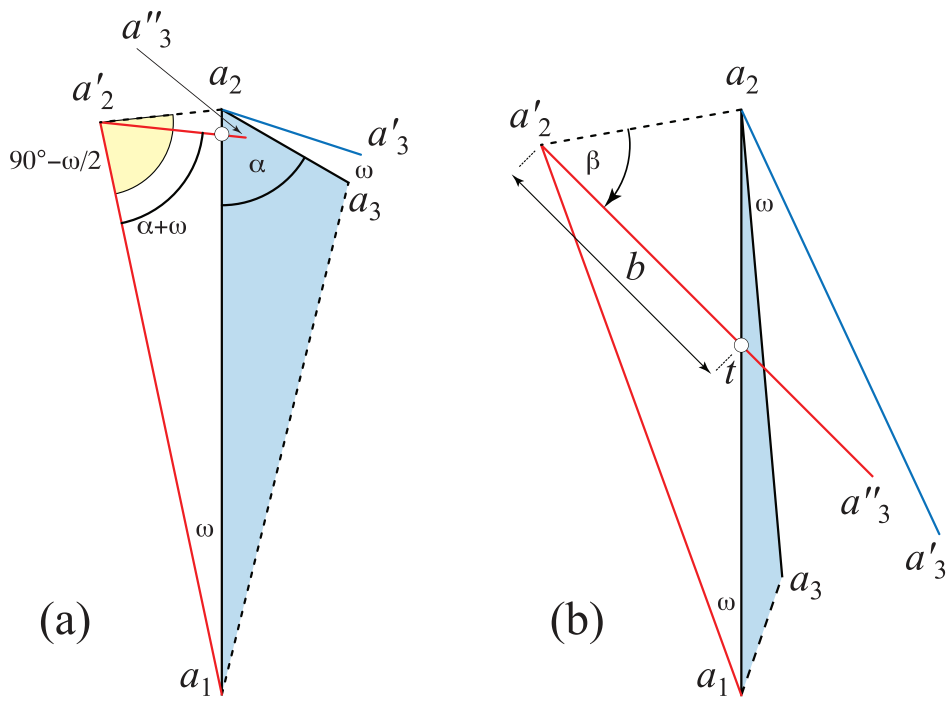

Figure 8 Similar to Fig. 6, unfolding the path $\Lambda = a_1, a_2, a_3$: rotation of a_2a_3 by ω about a_2 (blue), then rotation of $a_1a_2a_3'$ by ω about a_1 (red). Crossing point t is marked. (a) $\alpha, \omega = 60°, 12°$, $\alpha + 3\omega/2 = 78°$. (b) $\alpha, \omega = 5°, 20°$, $\beta = 55°$, $r, b = 0.8, 0.48$.

5.2 Two x-stretching lemmas

We achieve the conditions of Lemma 5 via x-stretching. First we show that x-stretching, like z-compression, reduces curvature at vertices.

▶ **Lemma 6.** *Horizontal x-stretching in any direction parallel to base B reduces the curvature $\omega(v)$ at any interior (non-base) vertex v below any given threshold ω.*

The proof is nearly identical to that of Lemma 4, except the normals at v approach lying in a vertical yz-plane rather than approaching a vertical z-vector.

[6] ∂_α is negative, driving α to 0, and ∂_ω is positive, driving ω to $\omega_{\max}$.

Proof. Let a_1, a_2, a_3 be a triangle of P incident to v, with $v = a_2$. Without loss of generality, translate P so that a_2 is placed at the origin, and scale the x-coordinates of every vertex by $s_x > 1$:

$$\begin{aligned} a_1 =& (s_x\, a_{1x}, a_{1y}, a_{1z}) \\ a_2 =& (0, 0, 0) \\ a_3 =& (s_x\, a_{3x}, a_{3y}, a_{3z}) \end{aligned}$$

So the stretch is along the x-axis. The normal vector to the triangle at a_2 is

$$\begin{aligned} \hat{n} =& (a_2 - a_1) \times (a_2 - a_3) \\ =& (c_x, s_x\, c_y, s_x\, c_z) \end{aligned}$$

where c_x, c_y, c_z are constants in the coordinates of the three vertices. The x-component of $\hat{n}$ is fixed independent of s_x, while the y- and z-components grow large with s_x. Therefore, as $s_x \to \infty$, $\hat{n}$ approaches lying parallel to the vertical yz-plane,

Because this is true for all triangles sharing the vertex $v = a_2$, all the normals of these incident triangles approach parallelism to the yz-plane. The Gauss map of these normals then encloses a vanishing thin area on $\mathbb{S}$. Therefore, by Proposition 0, the curvature at v approaches zero, and selection of a sufficiently small s_x will reduce the curvature at v below any given ω. ◀

We next prove that x-stretching can reduce the angle α at any particular vertex a_2, and at the same time increase the ratio r. This is how conditions (c) and (d) of Lemma 5 are satisfied.

▶ **Lemma 7.** *Let $\triangle = a_1a_2a_3$ be a triangle with a_1a_2 and a_2a_3 edges of P, while a_1a_3 might not be an edge (instead a diagonal of face F). Then horizontal x-stretching (parallel to the base of P) in a particular direction $\vec{\delta}$ eventually reduces the angle α at a_2 below any given threshold, and at the same time increases the ratio r as close as desired to* 1.

Note that "eventually" is necessary: α could increase before it decreases. See Fig. 11.

Proof. Place polyhedron P in a coordinate system so that the vertical yz-plane passes through a_1a_3, and a_2 lies in the $x > 0$ halfspace. The direction of x-stretching is then along a ray $\vec{\delta}$ perpendicular to the yz-plane and passing through a_2. See Fig. 9 for an explicit example.

It is clear from Fig. 11 that the angle α at a_2 approaches 0 as $s_x \to \infty$, and at the same time $r = \frac{|a_2a_3|}{|a_1a_2|}$ approaches 1 as $\triangle$ approaches isosceles. ◀

Now we show that the tighter conditions are achievable, including for Case 1.

▶ **Lemma 8** (Tighter Conditions Achievable). *The five conditions in Lemma 5 are achievable in Cases 1,2,3.*

Proof. The role of z-compression (Lemma 4) in Case 1 can be satisfied instead by Lemmas 6 and 7 because x-stretching reduces ω as well as α.

Cases 2 and 3 might both require adjustments in α, ω, r: reducing α and reducing $\omega = \max(\omega_1, \omega_2)$ to achieve $\alpha + 3\omega/2 < 90°$ and so $\beta > 0$, and increasing r beyond the length b in (d) of Lemma 5. Lemma 6 guarantees reducing ω, and Lemma 7 guarantees reducing α and moving r toward 1 (Fig. 11). Because $b < b_{\max} \approx 0.53$, eventually $r > b$. Thus both necessary conditions $\beta > 0$ and $r > b$ can be achieved, and so overlap is guaranteed. ◀

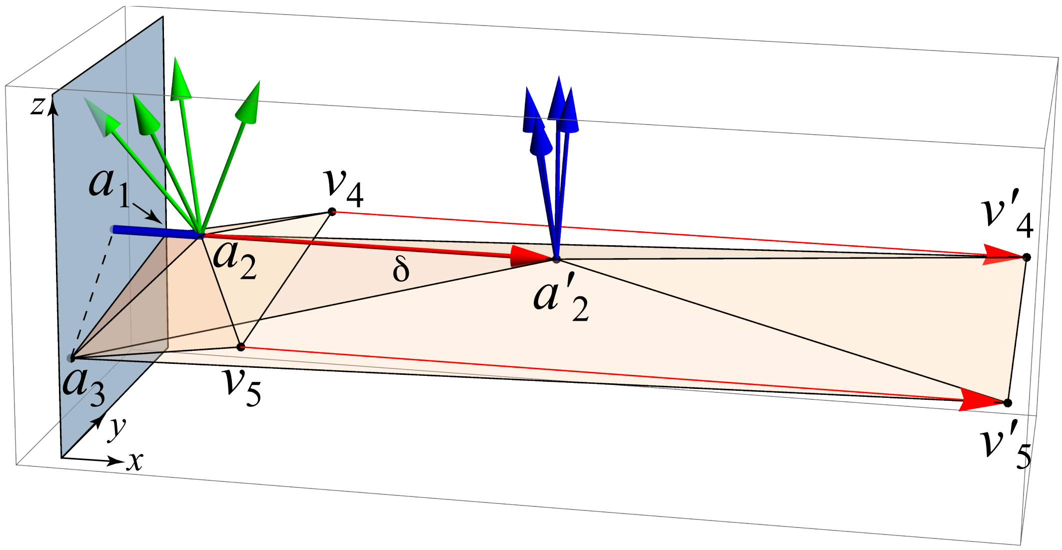

Figure 9 x-stretching all triangles incident to a_2 causes normal vectors at a'_2 to approach lying in the yz-plane.

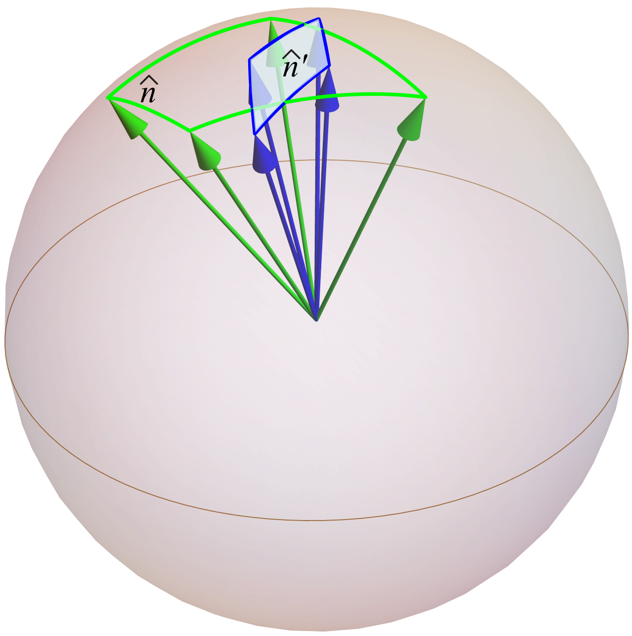

Figure 10 The $\hat{n}_i$ normal vectors from Fig. 9 before stretching (green) and $\hat{n}'_i$ after stretching (blue), on the Gaussian sphere $\mathbb{S}$.

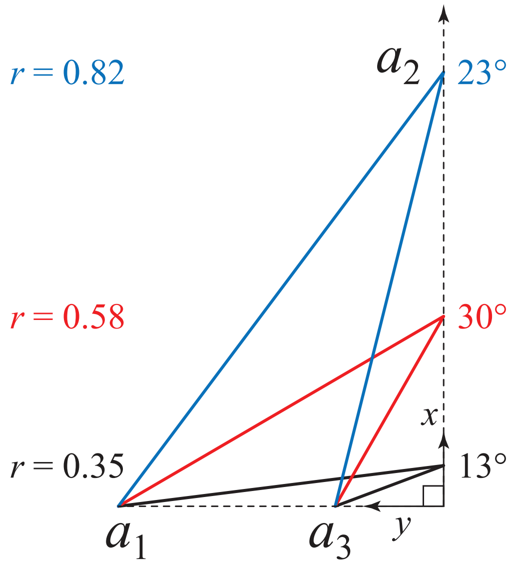

Figure 11 α can be nonmonotonic with x-stretching, whereas r approaches 1 monotonically (either from above or below 1)

.

5.3 Case 2 example: cube

Malkevitch's example of a combinatorial cube falls under Case 2. We start from the standard Schlegel diagram for a cube: one square inside another, and trapezoid faces between the squares. Lifting to a polyhedron retains the bottom and top squares, B and F respectively. B, F are disjoint, but F has no small angle: $\alpha = 90°$ and $\omega \approx 12°$, $\alpha + \omega \approx 102°$, so condition (b) of Lemma 5 fails. Identify one vertex of this square as a_2 and x-stretch by a factor of $s_x = 2$ perpendicular to the vertical plane through a_1, a_3. See Fig. 12. This squeezes B and F to 1×2 and 2×4 diamonds, so that the angle at a_2 reduces from $90°$, in this case to $2 \arctan(1/2) \approx 53°$. The curvatures $\omega_1 = \omega_2 \approx 6°$ are small enough so that all conditions of Lemma 5 are satisfied, and (strong) overlap achieved.

5.4 Case 3 example: hexagonal prism

Next we detail an example that falls under Case 3, a hexagonal pyramid. Let $v_1, \ldots, v_6$ be the vertices of $\mathcal{P}$ and v_7 the apex. A Schlegel diagram is shown in Fig. 13(a). No pair of faces is disjoint, but there are B, F pairs that share a single vertex. Let $B = v_6v_1v_7$ and $F = \triangle = v_3v_4v_7$ as illustrated. Then applying Tutte embedding and Maxwell-Cremona lifting, we arrive at the polyhedon P shown in (b) of the figure.

We label $a_1, a_2, a_3 = v_4, v_3, v_7$ respectively. Note a_3 is assigned to the vertex v_7 shared between B and F. The angle at a_2 is $\alpha \approx 79°$, and the curvatures $\omega_1 = \omega_2 \approx 24°$. So $\alpha + 3\omega/2 \approx 115°$ violates condition (c) of Lemma 5.

In preparation for x-stretching, place a vertical yz-plane through a_1, a_3, and project a_2 onto this plane, as in Fig. 14(a). Although stretching by a factor of 2 suffices, we illustrate $s_x = 4$ in Fig. 14(b) to highlight the changes. Now $\alpha \approx 35°$, $\omega_1, \omega_2 \approx 7°$, and $\alpha + 3\omega/2 \approx 46°$, satisfies condition (c). Fig. 14(c) shows that indeed overlap occurs.

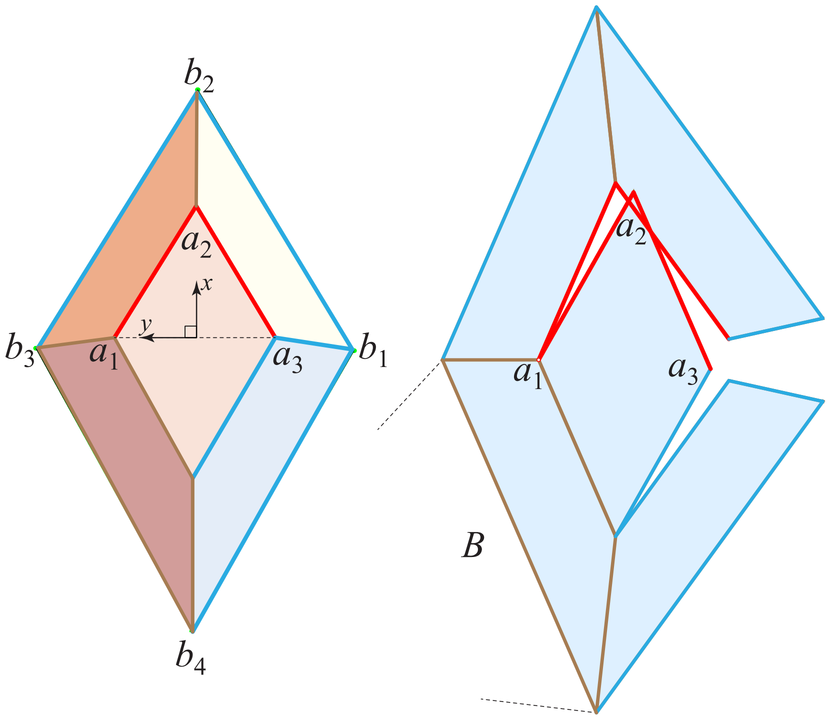

Figure 12 Unfolding of a combinatorial cube. The angle at α_2 is reduced from 90° by (vertical) x-stretching.

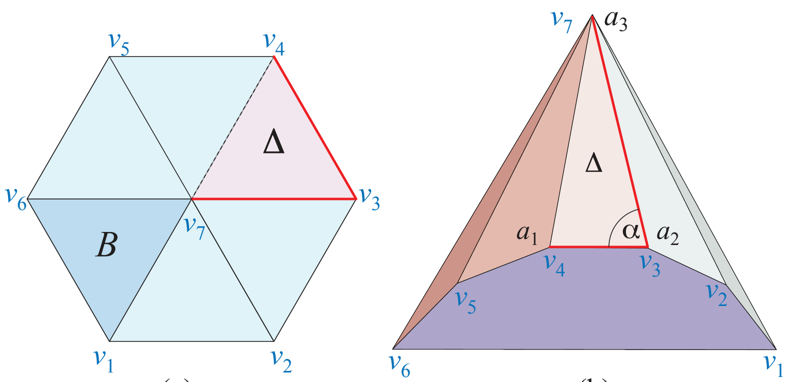

Figure 13 (a) Schlegel diagram of hexagonal prism. (b) Lifted polyhedron P over base $B = v_6v_1v_7$.

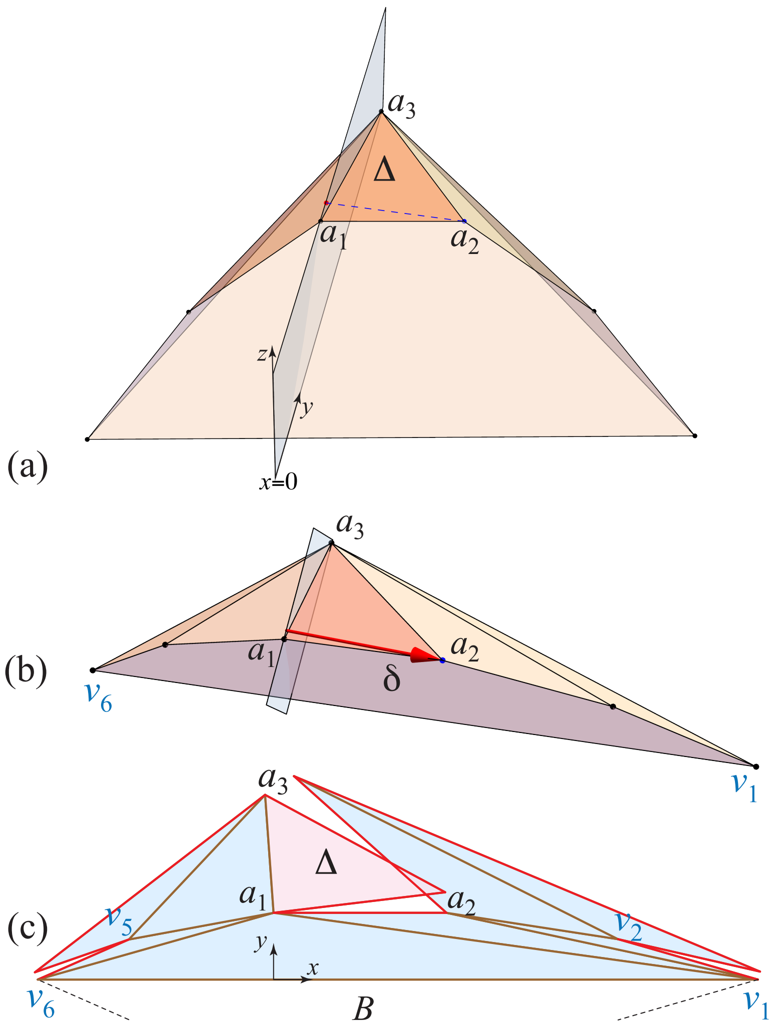

Figure 14 (a) Stretch direction $\vec{\delta}$ will be along the dashed segment orthogonal to the yz-plane containing a_1 and a_3. (b) After x-stretching by $s_x = 4$. (c) Unfolding with red cut edges results in overlap. Cut tree $T = (a_1, a_2, a_3)$, (a_3, v_1, v_2), (a_3, v_6, v_5).

6 Case 4

This leaves the case where there are no two disjoint faces, nor two faces that share just a single vertex: every pair of faces share two or more vertices. If two faces share non-adjacent vertices, they cannot both be convex. So in fact the condition is that each two faces share an edge. Then, it is not difficult to see that G can only be a tetrahedron, as the following argument shows.

Start with Euler's formula, $V - E + F = 2$, where V, E, F are the number of vertices, edges, and faces respectively. Each vertex v must be incident to exactly three faces, because, if v has degree ≥ 4, then each non-adjacent pair of faces incident to v cannot share an edge. So $3V = 2E$. Substituting into Euler's formula yields $F = 2 + E/3$.

Because each pair of faces share an edge, $F(F-1)$ double counts edges:[7] $2E = F(F-1)$. Substituting,

$$\begin{aligned} F &= 2 + E/3 \\ E &= F(F-1)/2 \\ F &= 2 + F(F-1)/6 \\ 0 &= F^2 - 7F + 12 \\ 0 &= (F-3)(F-4) \end{aligned}$$

The two solutions of this quadratic equation are $F = 3$, which cannot form a closed polyhedron, and $F = 4$. The tetrahedron is the only polyhedron with four faces, and indeed $F = 4$ implies $V = 4$ and $E = 6$.

So the only case remaining is a tetrahedron. But it is well known that the thin, nearly flat tetrahedron unfolds with overlap: Fig. 15. And since there is only one tetrahedron combinatorial type, this completes the inventory.

7 Main theorem revisited

We summarize the proof of the main theorem below.

▶ **Theorem 1.** *Any combinatorial convex polyhedron $\mathcal{P}$, given by a 3-connected planar graph G, can be realized as a convex polyhedron P in $\mathbb{R}^3$ whose 1-skeleton has a spanning cut-tree T such that the edge-unfolding of $P \setminus T$ strongly overlaps in the plane.*

Proof. Cases 1, 2 and 3 are covered by Lemmas 5 and 8, all via x-stretching. Case 4 is established by the overlapping thin tetrahedron (Fig. 15). As the four cases exhaust all possibilities, the theorem is proved. ◀

So together with Ghomi's result,[8] any combinatorial polyhedron type can be realized to edge-unfold and avoid overlap, or realized to edge-unfold with overlap by Theorem 1.

8 Open problems

(1) That each of the three parameters α, ω, r moves under x-stretching in the "right" direction for overlap, suggests there could be a simpler proof of Lemma 8 and therefore of Theorem 1.

[7] Similar logic is used to form Szilassi's polyhedral torus.
[8] See [14] for a different proof of [5].

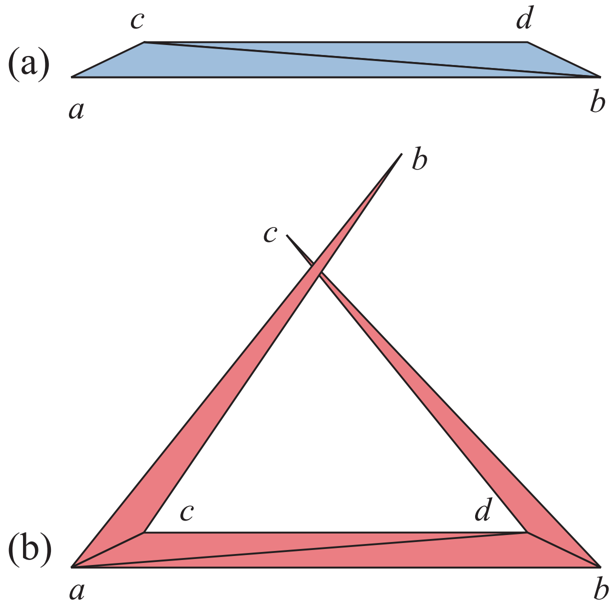

Figure 15 Fig. 28.2 in [4]: tetrahedron overlap. Blue: exterior. Red: interior. Cut tree $T = abcd$.

(2) Is there a combinatorial Hamiltonian polyhedron $\mathcal{P}$ whose every metric realization P and every Hamiltonian path T, $P \setminus T$ unfolds to a net? This restricts Malkevitch's question to Hamiltonian polyhedra $\mathcal{P}$, and restricts T to a Hamiltonian path, producing a *zipper unfolding* [3]. Note that some convex polyhedra are not Hamiltonian, e.g., the rhombic dodecahedron. Restricting to 4-connected graphs G guarantees that G is Hamiltonian [18].

(3) We earlier described our result as: $\mathcal{P} \to P \to \bar{P} \to$ Unfold/Overlap. Ghomi's result is stronger, in that he starts with a metrically realized polyhedron $P \to \bar{P} \to$ Unfold/Non-verlap. Can Theorem 1 be strengthened to achieve: $P \to \bar{P} \to$ Unfold/Overlap, where $P \to \bar{P}$ is an affine transformation?

Acknowledgements. I benefitted from discussions with Joseph Malkevitch and Richard Mabry, from audience questions at *CCCG* [10], and from comments and corrections from four referees.

References

1 Therese Biedl, Anna Lubiw, and Michael Spriggs. Cauchy's theorem and edge lengths of convex polyhedra. In *Workshop Algorithms Data Struct. (WADS)*, pages 398–409. Springer, 2007.

2 Hsien-Chih Chang, Jeff Erickson, and Chao Xu. Detecting weakly simple polygons. In *Proc. 26th ACM-SIAM Symp. Discr. Algorithms (SODA)*, pages 1655–1670. SIAM, 2014.

3 Erik D. Demaine, Martin L. Demaine, Anna Lubiw, Arlo Shallit, and Jonah Shallit. Zipper unfoldings of polyhedral complexes. In *Proc. 22nd Canad. Conf. Comput. Geom.*, pages 219–222, August 2010.

4 Erik D. Demaine and Joseph O'Rourke. *Geometric Folding Algorithms: Linkages, Origami, Polyhedra*. Cambridge University Press, 2007.

5 Mohammad Ghomi. Affine unfoldings of convex polyhedra. *Geom. Topol.*, 18(5):3055–3090, 2014.

6 Richard Goldstone and Robert Suzzi Valli. Unfoldings of the cube. *College Math. J.*, 50(3):173–184, 2019.

7 Joseph O'Rourke. Dürer's problem. In Marjorie Senechal, editor, *Shaping Space: Exploring Polyhedra in Nature, Art, and the Geometrical Imagination*, pages 77–86. Springer, 2013.

8 Joseph O'Rourke. Unfolding convex polyhedra via radially monotone cut trees. *arXiv:1607.07421*, 2016. `https://arxiv.org/abs/1607.07421`.

9 Joseph O'Rourke. Edge-unfolding nearly flat convex caps. In *Proc. Symp. Comput. Geom. (SoCG)*, volume 99, pages 64:1–64:14. Leibniz Internat. Proc. Informatics, June 2018. Full version: `https://arxiv.org/abs/1707.01006`.

10 Joseph O'Rourke. Every combinatorial polyhedron can unfold with overlap. In *Proc. 35th Canad. Conf. Comput. Geom.*, pages 257–263, August 2023.

11 Manuel Radons. Edge-unfolding nested prismatoids. *Comput. Geom.*, 116:102033, 2024.

12 Jürgen Richter-Gebert. *Realization Spaces of Polytopes*. Springer, 2006.

13 André Schulz. *Lifting planar graphs to realize integral 3-polytopes and topics in pseudo-triangulations*. PhD thesis, Univerität Berlin, 2008.

14 Gözde Sert and Sergio Zamora. On unfoldings of stretched polyhedra. *arXiv:1803.09828*, 2018. `https://arxiv.org/abs/1803.09828`.

15 Geoffrey C. Shephard. Convex polytopes with convex nets. *Math. Proc. Camb. Phil. Soc.*, 78:389–403, 1975.

16 J. J. Stoker. Geometrical problems concerning polyhedra in the large. *Comm. Pure Appl. Math.*, 21:119–168, 1968.

17 Christopher Tuffley. Counting the spanning trees of the 3-cube using edge slides. *arXiv:1109.6393*, 2011. `https://arxiv.org/abs/1109.6393`.

18 William T. Tutte. On Hamiltonian circuits. *J. London Math. Soc.*, 1(2):98–101, 1946.

19 William T. Tutte. How to draw a graph. *Proc. London Math. Soc.*, 13(52):743–768, 1963.